2017

Incorporating Passive Compliance for Reduced Motor Loading During Legged Walking

Akhil Sai Pabbu
Wright State University

INCORPORATING PASSIVE COMPLIANCE FOR REDUCE MOTOR LOADING DURING LEGGED WALKING

A thesis submitted in partial fulfillment of the
requirements for the degree of
Master of Science in Electrical Engineering

By

AKHIL SAI PABBU
B.Tech, Jawaharlal Nehru Technological University, India, 2015

2017
Wright State University

WRIGHT STATE UNIVERSITY

GRADUATE SCHOOL

July 19, 2017

I HEREBY RECOMMEND THAT THE THESIS PREPARED UNDER MY SUPERVISION BY Akhil Sai Pabbu ENTITLED 'Incorporating Passive Compliance for Reduce Motor Loading During Legged Walking' BE ACCEPTED IN PARTIAL FULFILLMENT OF THE REQUIREMENTS FOR THE DEGREE OF Master of Science in Electrical Engineering.

Luther R. Palmer III, Ph.D.
Thesis Director

Brian Rigling, Ph.D.
Chair, Electrical Engineering

Committee on Final Examination

Luther R. Palmer III, Ph.D.

Zach Fuchs, Ph.D.

Xiaodong (Frank) Zhang, Ph.D.

Robert E. W. Fyffe, Ph.D.
Vice President for Research and
Dean of the Graduate School

ABSTRACT

Pabbu, Akhil Sai. M.S.E.E. DEPARTMENT OF ELECTRICAL ENGINEERING, Wright State University 2017. **'Incorporating Passive Compliance for Reduced Motor Loading During Legged Walking'**

For purposes of travelling on all-terrains surfaces that are both uneven and discontinuous, legged robots have upper-hand over wheeled and tracked vehicles. The robot used in this thesis is a simulated hexapod with 3 degrees of freedom per leg. The main aim is to reduce the energy consumption of the system during walking by attaching a passive linear spring to each leg which will aid the motors and reduce the torque required while walking. Firstly, the ideal stiffness and location or the coordinates for mounting the spring is found out using *gradient based algorithm* called **'Simultaneous Perturbation and Stochastic Approximation Algorithm' (SPSA)** on a flat terrain using data from a single walking step. Motor load is approximated by computing the torque impulse, which is the summation of the absolute value of the torque output for each joint during walking. Once the ideal spring and mount is found, the motor loading of the robot with the spring attached is observed and compared on three different terrains with the original loading without the spring. The analysis is made on a single middle leg of the robot, which is known to support the highest load when the alternating tripod gait is used. The obtained spring and mounting locations are applied to other legs to compute the overall energy savings of the system. Through this work, the torque impulse was decreased by 14 % on uneven terrain.

Keywords: *Legged robots, Energy optimization in legged robots, Optimization using SPSA, Gradient based optimization, Spring placement on a hexapod, Energy cost, Torque distribution.*

Table of Contents:

List of Figures

Chapter 1: Introduction

1.1 Legged Walking:

There are many forms of locomotion available for robotic system, one of which is legged walking, others being on wheels, hovering etc. This thesis report consists of a study of how legged walking can be improved on a hexapod system by reducing of energy consumed while walking.

A legged hexapod has a general construction of six legs of three segments each: coxa, femur, and tibia. For a hexapod to walk with stability, the angle and position of all the legs and their parts need to be controlled according to a coordinated gait pattern.

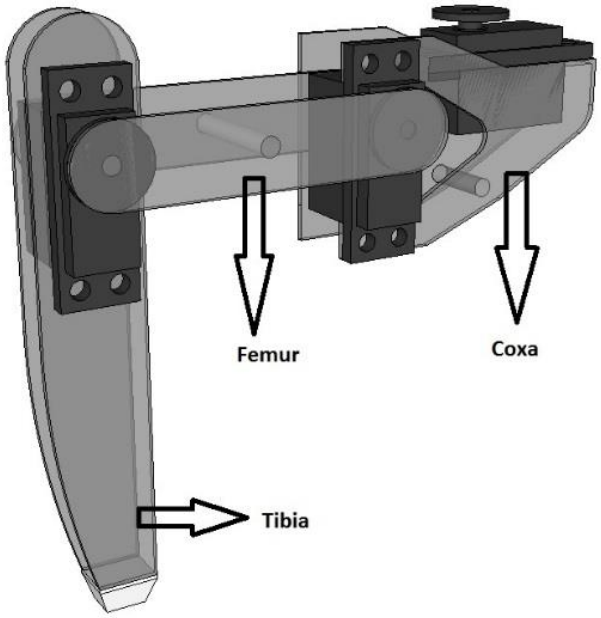

;

Figure 1.1: Figure explaining different parts of the robot leg

Legged walking has a significant advantage when the robot needs to navigate on a rough terrain. The lift-and-place method used by the legs of the robot can make it robust to

unwanted disturbance as they do not need continuous contact with the ground. This has attracted considerable attention in the past decade. There are several other benefits of legged walking: efficient in maintaining stability with three of more legs, usage of gaits for locomotion so the speed of locomotion can be varied easily, legs do less damage to the terrain than tracks and wheels. Also, the height of the robot can be changed according to the constraints if the leg joints are built to have sufficient degrees of freedom.

Primary disadvantages of legged robots are the complexity of the systems and energy usage. This thesis seeks to address the latter concern by incorporating passive compliance in each leg.

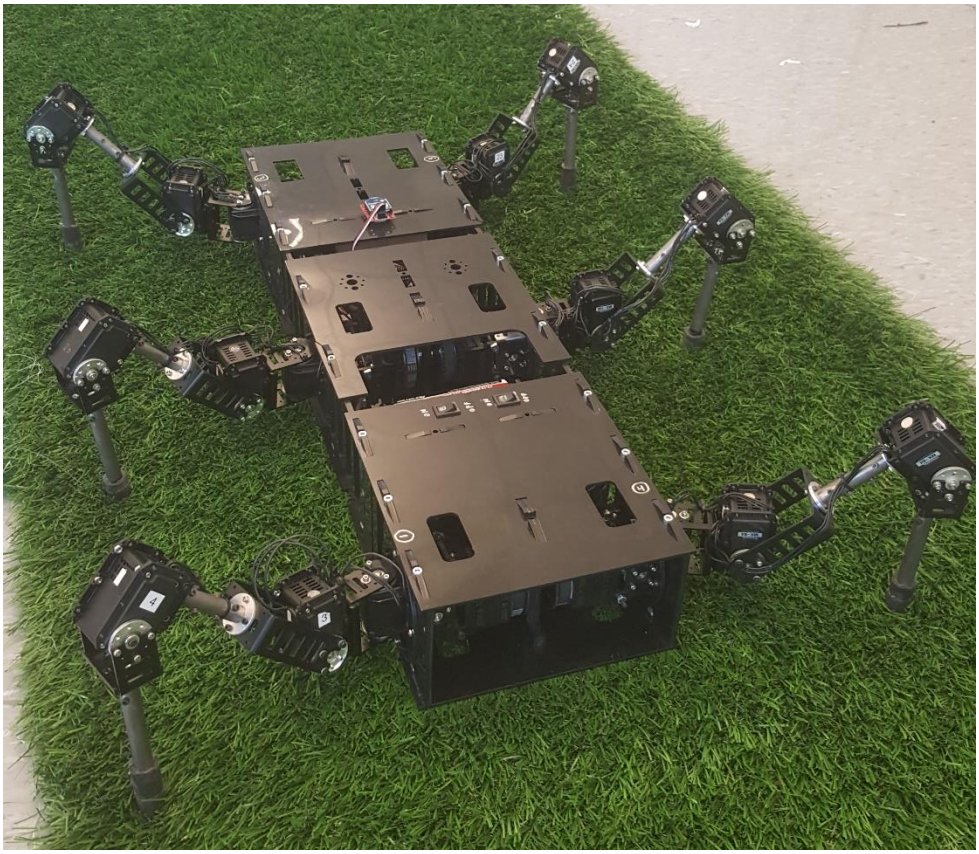

Figure 1.2: Picture of Hexapod Robot discussed in this thesis

1.2 Hexapod gaits:

During the walking of a legged robot, there is a crucial problem of generation and control of the sequence of placing and lifting the legs such that at any instant, the body

should be stable and capable of moving from one position to another. The generation and sequence of such leg motion is called Gait. Gaits are repeated periodically on a robot for successful locomotion from one point to another.

The hexapod robot has six legs for locomotion, at least three of which need to be on the ground at any point of time to ensure stable locomotion. There are three main gaits used by a hexapod robot: wave gait, ripple gait and tripod gait; each ensuring system stability always.

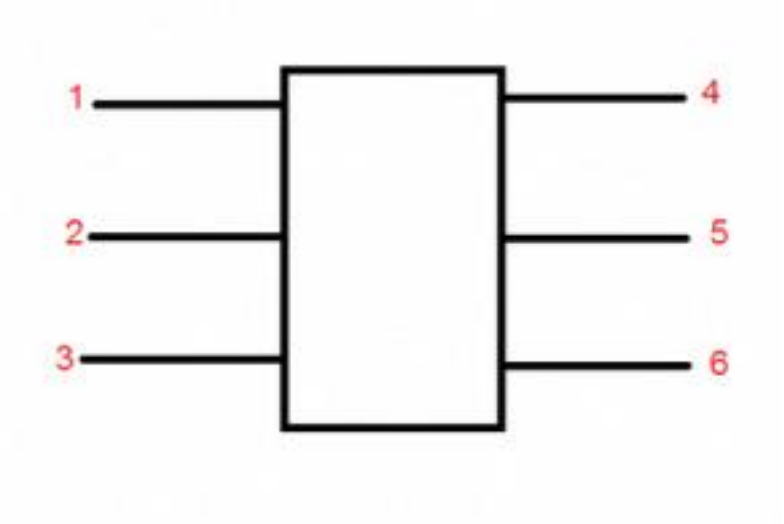

Figure 1.3: Figure explaining the leg numbering of the robot

1.2.1 Tripod gait:

The walking stride of the tripod gait in a hexapod robot consists of two individual steps. At any instance, at least three legs of the robot stand on the ground providing support and force to push the body forward while the other three legs swing forward to take the stance position. Considering the legs of the robot are numbered as shown in Figure 1.3, legs 1, 3, and 5 begin in a stance (on the ground) position and legs 2, 4 and 6 swing forward in flight. As the legs 2, 4, and 6 touch the ground, they change to stance position while legs 1, 3, and 5 swing forward in flight. Thus the hexapod moves forward in a cycle of two simple steps in tripod gait. The foot fall pattern of Tripod gait is shown in Figure 1.4

1.2.2 Wave gait:

The walking mechanism of the wave gait in a hexapod robot consists of six steps. At any instance, at least five legs of the robot stand on the ground providing support and force to push the body forward while the other leg swings forward to take the stance position. Considering the legs of the robot are numbers as shown in Figure 1.3, legs 1, 2, 4, 5 and 6 begin in a stance position and leg 3 swings forward. Then, leg 2 swings forward while the others are in the stance phase. Then, leg 1 swings forward, followed by legs 6, 5 and 4 while the other legs are in stance phase for each step. Thus, to complete one cycle of a Wave gait, six legs take six individual steps each. The foot fall pattern of Wave gait is shown in Figure 1.4

1.2.3 Ripple gait:

The walking mechanism of the ripple gait in a hexapod robot consists of six steps. At any instance, at least four legs of the robot stand on the ground providing support and force to push the body forward while the other two legs swing forward to take the stance position. Considering the legs of the robot are numbers as shown in Figure 1.3, legs 1, 2, 5 and 6 begin in a stance position and legs 3 and 4 swings forward. While leg 4 is still in swing position leg 2 begin to swing. Leg 6 start swinging as soon as leg 4 touches down. This pattern is followed by the legs to complete the gait. Thus, to complete one cycle of a Ripple gait, it takes 3 steps. The foot fall pattern of Ripple gait is shown in Figure 1.4

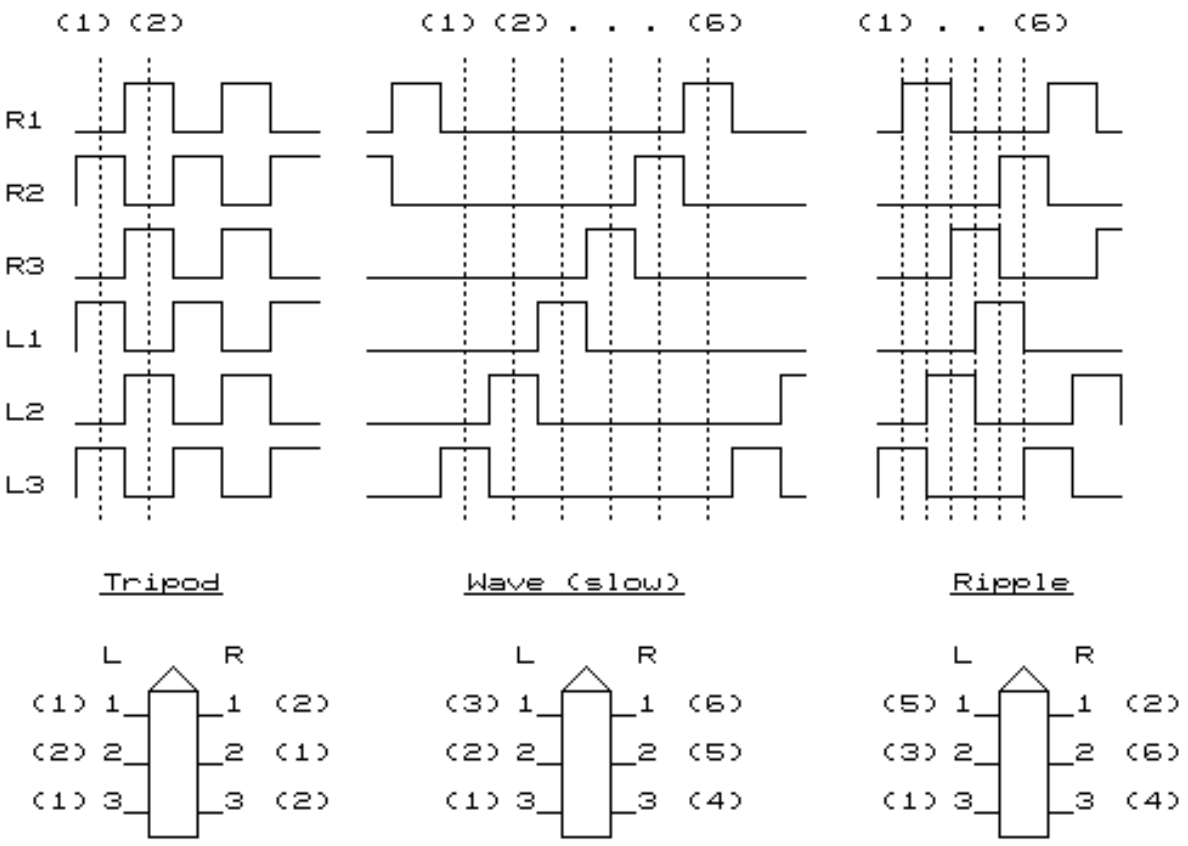

Figure 1.4: Figure shows different gait patterns

1.3 Hexapod Stride

While walking, each leg of the hexapod repetitively goes through two phases: stance and swing. These two phases together complete one cycle of the hexapod stride. The time periods for which the legs stay in stance phase and swing phase are called stance period and swing period, respectively. These are controlled by an aspect called duty factor, which is the ratio of the stance period of the leg to its total stride period. For example, if the legs move in stance and swing phases for equal amount of times, that is, if the stance period is equal to the swing period, the duty factor of the gait is computed to be 0.5. If the leg is in stance for 75% of the entire stride, the duty factor is 0.75. The duty factor ranges

between 0 and 1, and it is the same value for all the legs of the hexapod while the system moves in a gait.

1.3.1 Stance period:

This is the time period for which the leg of the hexapod is in contact with the ground. During locomotion, the legs that are in the stance phase help to provide stability to the system while pushing the body forward. Together, they form a support polygon that is used to calculate the stability margin of the body in its current position.

Figure 1.5: Figure shows the stance phase of the leg during a stride

1.3.2 Swing period:

This is the time-period for which the leg of the hexapod is swinging forward. During locomotion, the swing period of the legs is used to bring the legs forward by lifting them off the ground and moving them ahead of the leg-body joint so as to take the stance phase at the beginning of the next cycle.

Figure 1.6: Figure shows the swing phase of the leg during a stride

1.3.3 Stride Period:

This is the total time period that constitutes a swing phase and stance phase. That is, the leg completes a full 360-degree rotation at the leg-body joint in one stride period. The stride period of the body is decided based on the velocity with which the system is moving forward. The duty factor is then used to compute the swing and stance periods.

All the legs on the system operate using the same values for each of the above time periods. Thus, the gait of the hexapod is changes either by varying the body velocity, or the duty factor. This report mainly details the work based on a tripod gait using a 75% duty factor.

1.4 Other Hexapod Robots:

The more legs that a system has, the less challenging it is to maintain stability. Specifically, hexapods possess greater static stability both while standing and while walking over 4-legged robots. Most of these hexapod robots are inspired from biological

species, but are not intended to explicitly mimic these systems. A few of these hexapod robots are described below.

1.4.1 RHex:

This is a design inspired from biological species. It does not have a multi-joint leg and also was the inspiration for the miniature robot called **The DynaRoACH** robot which is only 10 cm in length and weighs 24 grams. This system can travel 14 body lengths per second [3].

Figure 1.7: RHex robot

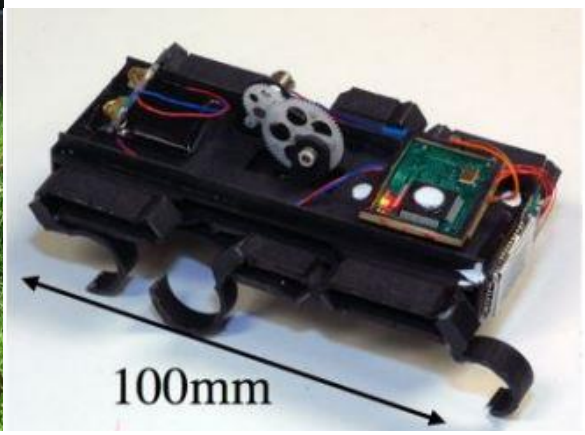

Figure 1.8: DynaRoach Robot

This design is described as under actuated, as there are passive joints that are not explicitly controlled. As there is not much joint movements or complex controlling. Due to its small size, the DynaRoach robot's legs are made out of polyelastic materials which makes it easier to tune the stiffness of its legs. By adjusting the stiffness, the stability of the robot can be maintained [4].

1.4.2 Lauron V:

Lauron is a biologically-inspired robot which mimics the walking behavior of the stick insect Carausius Morosus. The research on Lauron started in early 1990s and led to the development of Lauron I which is in contrast with the present Lauron V. Lauron V has the artificial neural network. The name of the robot LAURON which actually stands for *LAUf Roboter Neuronal Gesteuert* meaning *neural controlled walking robot* [5].

This robot was actually developed to study and realize the statically stable walking in rough terrain. Due to its flexible behavior walking control, this robot can adopt itself to different terrains. And, its robust design and multiple joint legs which gives more degrees of freedom helps it to maintain stable locomotion under various circumstances [6].

Figure 1.9: Lauron V

The robot used in this thesis is custom built and is rectangular as shown in figure below. By using the spring, the motor load of the dominant joint during walking is optimized to 28%. These results are obtained by using the leg #2 on a flat terrain but by extrapolating these results to other legs, the efficiency can be increased. The same robot is then tested on different terrains and the results are compared among these terrains.

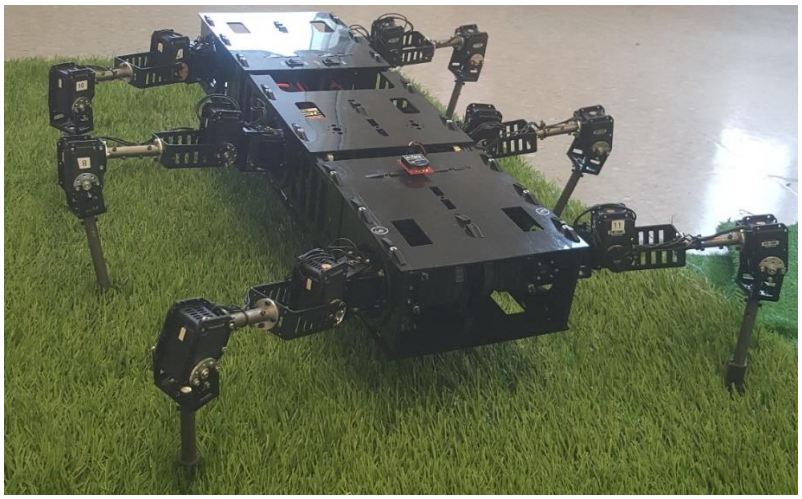

Figure 1.10: Hexapod Robot discussed in this thesis

1.5 Contribution:

There have been various methods to optimize the energy of a hexapod robot. Some of them have adopted for an efficient body shape and design, few have adopted for a different leg design and few other choose a design which gives them a better and efficient zero torque angle.

In same way, this thesis consists of a different approach of using springs to assist the motors and reduce the total torque required by them for walking. As the data used in all the simulations to get the lowest cost is based on a robot which is already build, this is not the most efficient way of placing the spring as the priority here has been given to an easy design than getting to a spring placement that gives lowest cost. By making few changes to the SPSA algorithm used in this thesis this concept can be adopted to optimize the energy consumption of any state of the art hexapod robot that are present.

The big picture will be adopting this concept on robots which are not just hexapods, but also bipeds, quadrupeds and other leg arrangements.

Chapter 2: Approach

2.1 Spring Attachment:

This section is the most important part of this thesis due to following factors

1. It helps to understand how various torques act on the leg of the robot.
2. It shows how the spring is mounted on the robot
3. It explains the search space around the robot used for SPSA algorithm
4. It shows the working of different types of springs

Points to be noted:

■ color indicates the torque applied by the motor

■ color indicates the torque applied by the spring or the spring force

Assume that the duty cycle for this stride period is 75%

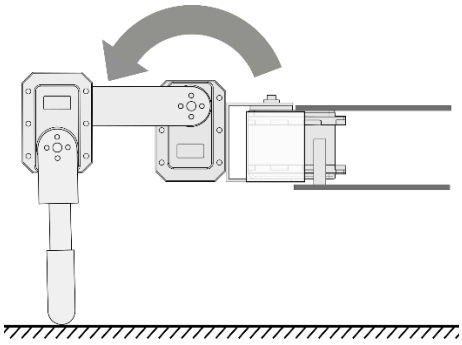

Figure 2.1: [1a] Torque exerted by the motor to support body weight of the robot

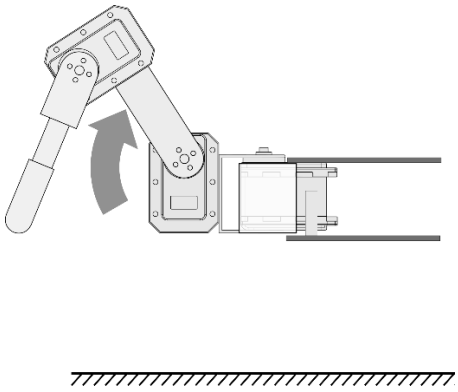

Figure 2.2: [1b] Torque required to lift the leg up in the air during Swing phase

Picture [1a] gives an idea of how much torque is required to support the body compared to amount of torque required to lift the leg in air in picture [1b]. For a duty cycle of 75%, more part of the stride period is stance phase so more torque is required to support the weight of the robot. The concept of using a spring is to reverse the amount of torque required in Stance phase and swing phase.

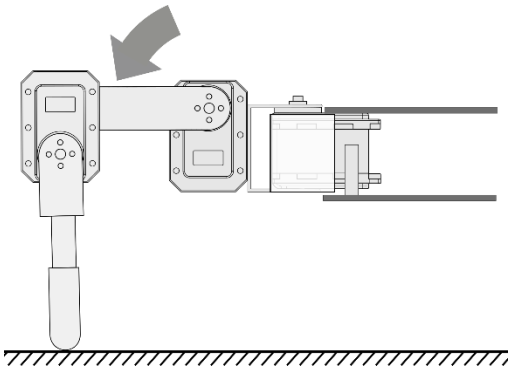

Figure 2.3: [2a] Desired torque to support the body of the robot

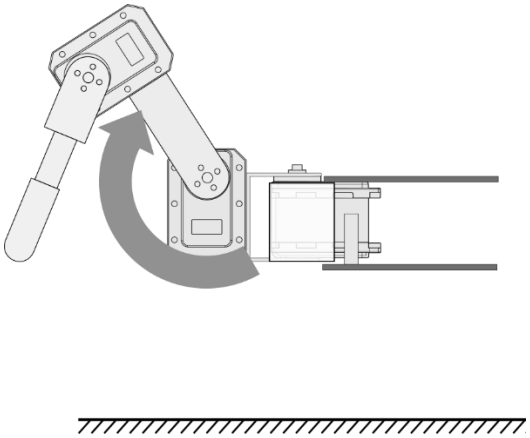

Figure 2.4: [2b] Desired torque to lift the leg during Swing phase

The torque shown in picture [2a] and [2b] is the desired torque that must be applied by the motor. This can be achieved by mounting a spring. As the stance phase covers more part of the stride period, the torque required in that phase should be less to achieve more efficiency.

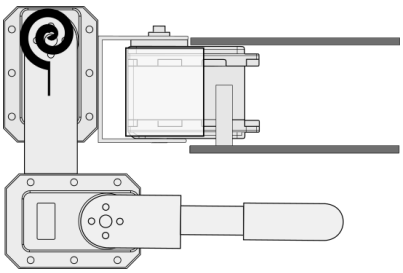

Figure 2.5: [3a] Mounting position of the Torsional Spring

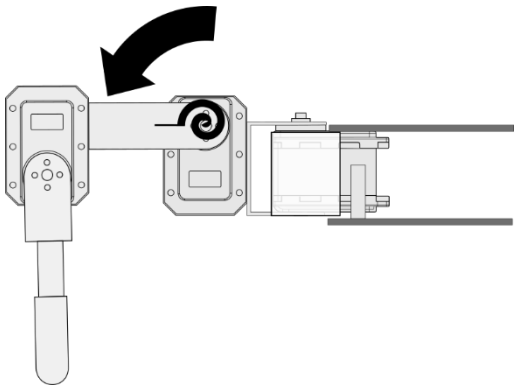

Figure 2.6: [3b] Torque applied by the torsional spring during Stance phase

One way of achieving this efficiency is by mounting the spring as shown in picture [3a]. So that it applies a torque as shown in picture [3b] there by reducing the torque required during stance phase.

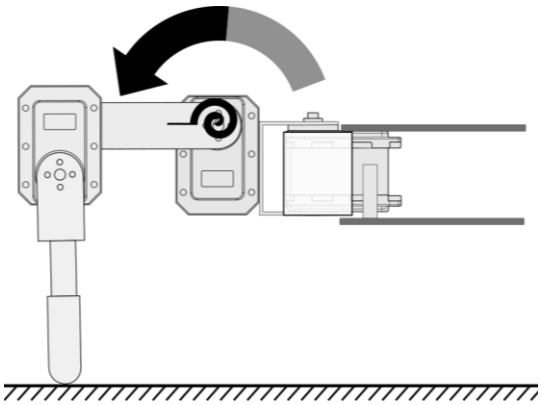

Figure 2.7: [4a] Total torque applied by spring and motor during Stance phase

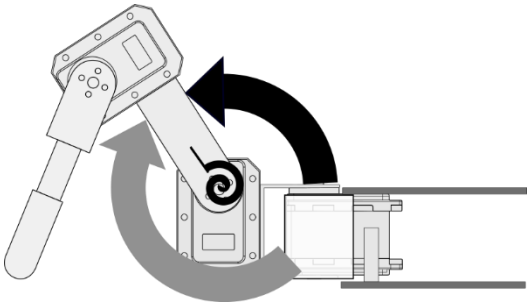

Figure 2.8: [4b] Total torque applied by the motor to lift the leg during Swing phase

Total torque applied by the spring and motor to support the weight of the robot is shown in picture [4a] which is similar to the desired one. But when it comes to picture [4b], the torque required to lift the leg and oppose the spring torque is very high, more than the desired. This type of spring will hurt the system than helping it.

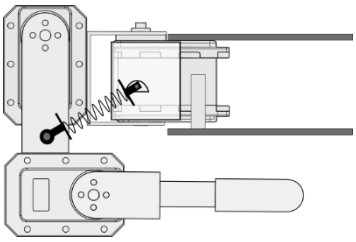

Figure 2.9: [5a] Placement of the linear spring

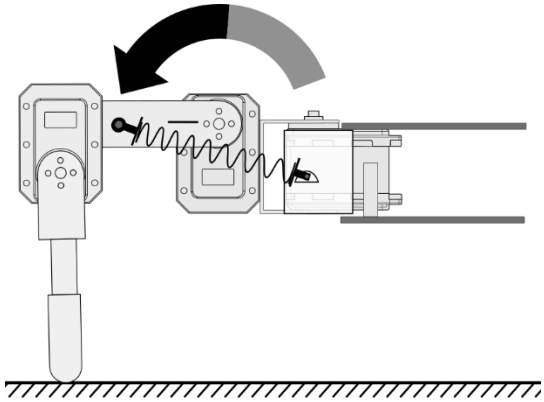

Figure 2.10: [5b] Total Torque applied by spring and motor

Due to the failure of torsional spring, a linear spring is mounted as shown in picture [5a]. This spring is expected to overcome the drawback of the torsional spring. Similar to the torsional spring, the linear spring also supports the weight of the robot as shown in picture [5b].

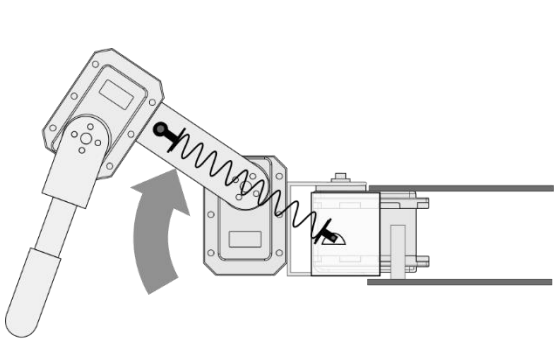

Figure 2.11: [6a] Torque applied by the motor at Zero-torque angle

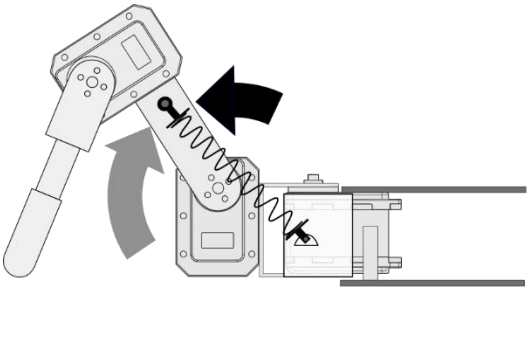

Figure 2.12: [6b] Torque required by the motor to lift the leg and support the opposing spring torque

But one point which cannot be possible in torsional spring is the zero-torque angle. A position in which the two anchors of the spring, the axis on which the leg rotates all stay in a line. At this point, the spring force is cancelled out by the axis. Therefore, only force acting on the leg is the torque applied by the motor. This position is explained through picture [6a]. Even at an angle which is greater than the zero-torque angle, the force applied by the spring will be less as it the rectangular component of the actual force. Due to which the total force applied by the motor to support the weight of the leg and counter the torque applied by the spring is very low. This case is shown in picture [6b].

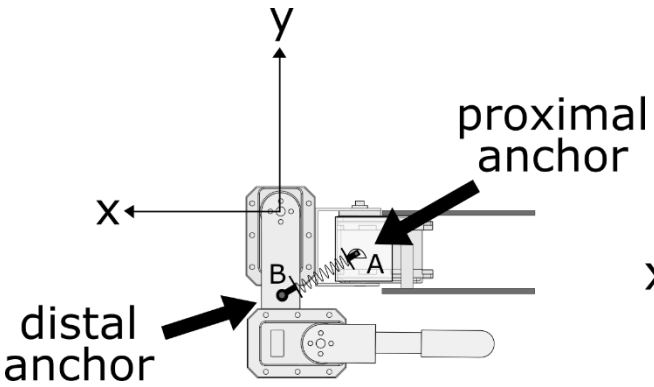

Figure 2.13: [7a] Figure showing the Co-ordinate system of the search space used for SPSA algorithm

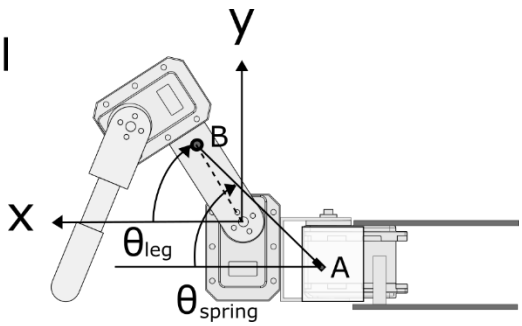

Figure 2.14: [7b] Spring and leg angles with respect to search space

Picture [7a] shows the direction of X-axis and Y-axis for the search space used in SPSA algorithm. 'A' and 'B' are the two ends of the spring or the anchor points of the spring. Point 'A' is the proximal anchor and point 'B' is the distal anchor. All the notations in the MATLAB code and SPSA are based on 'A' and 'B' points. Picture [7b] is used as the reference for the terminology for the equations used to calculate all the parameters in the user built function *getSpringtorque()*.

Equations:

The initial spring length, d_0, is computed at the mounting location of the spring as

$$d_0 = \sqrt{\left(a_x - b_{x,init}\right)^2 + \left(a_y - b_{y,init}\right)^2}$$

The distal anchor position, b, moves as the leg moves, and is computed as a rotation about the leg angle, θ_{leg} by

$$b = \begin{bmatrix} \cos(\theta_{leg}) & \sin(\theta_{leg}) \\ -\sin(\theta_{leg}) & \cos(\theta_{leg}) \end{bmatrix} \begin{bmatrix} b_{x,init} \\ b_{y,init} \end{bmatrix}$$

Note that the proximal anchor position does not change. The current spring length, d, is computed by

$$d = \sqrt{(a_x - b_x)^2 + (a_y - b_y)^2}$$

The scalar spring force is computed using the spring constant, k, as

$$f_{spring} = k(d - d_0)$$

The direction of the spring force is

$$\theta_{spring} = atan2(b_y - a_y, b_x - a_x)$$

and the spring force vector is computed by

$$f^x_{spring} = f_{spring}\cos(\theta_{spring}), \text{ and}$$

$$f^y_{spring} = f_{spring}\sin(\theta_{spring})$$

Finally, the spring-generated torque is the cross product of the b vector and the spring force vector:

$$\tau_{spring} = b\ x\ f_{spring} = b_x f_y + b_y f_x$$

After mounting the spring, the equation for total torque can be given by

$$I_\tau = \sum \left| \tau_{motor} + \tau_{spring} \right|$$

where τ_{motor} is the torque provided by the motor and τ_{spring} is the torque provided by the spring.

2.2 SPSA:

The Simultaneous Perturbation Stochastic Approximation Algorithm (SPSA) is an efficient gradient based algorithm used to find the minimum local cost for optimization over a set of cost functions (response surfaces). The details of the algorithm are as given below.

For instance, assume that there is a 2-D search space which need to be optimized. Therefor $p = 2$, where 'p' is the dimension of the search space. The cost *'J'* is a function of *'θ'* where size of *'θ'* depends on value of *'p'*. In this case,

$$\theta = [\theta_1 \quad \theta_2]$$

where size of *'θ'* and *'c'* is [1 x p]. The accuracy of the system depends on number of iterations *'j'*, value of 'λ' which is the *'step size'* and the value of 'c' which is the *'viewing distance'.* Guidelines for choosing the values for 'λ' and 'c' are given in the next section.

Once we chose values for 'λ', 'c' and initial 'θ' i.e. $\theta_{j=1}$, the SPSA calculates the gradient for those values by

$$g_i(\theta(j), j) = \frac{J_n\big(\theta(j)\big) + c_j \Delta(j)) - J_n(\theta(j) - c_j \Delta(j))}{2 c_j \Delta_i(j)}$$

where $c_j > 0$ for all j and

$$\Delta(j) = \begin{bmatrix} \Delta_1(j) \\ \vdots \\ \Delta_p(j) \end{bmatrix}$$

is a random perturbation vector. The components of the vector Δ(j) should be independently generated from a zero-mean probability distribution and one theoretically valid choice is to use a Bernoulli ± 1 distribution for each ± 1 outcome. In this way, the $\theta(j) \pm c_j \Delta(j)$ lie in a known bounded region. Note that if p =2 , then the Δ(j) are the corners of a unit square so for each j

$$\Delta(j) \in \left\{\begin{bmatrix}1\\1\end{bmatrix}, \begin{bmatrix}1\\-1\end{bmatrix}, \begin{bmatrix}-1\\1\end{bmatrix}, \begin{bmatrix}-1\\-1\end{bmatrix}\right\}$$

In general, there are 2^p possible $\Delta(j)$values.

After the gradient is calculated, the 'θ' value is updated as follows

$$\theta(j+1) = \theta(j) - \lambda_j g(\theta(j), j)$$

Where $g(\theta(j), j) \epsilon \Re^p$ is an estimate of $\nabla J(\theta(j))$ at θ(j).

In this thesis, SPSA is used to optimize the total torque required by the motor for walking. This is done with the help of a spring placed between the body and the Coxa of the leg. The total torque changes with the position of the spring. In a two-dimensional coordinate system, the position of the spring can be described using four values: (x, y) of the distal joint, (x, y) of the proximal joint. Thus, the response function used in this thesis is a 4-D search space.

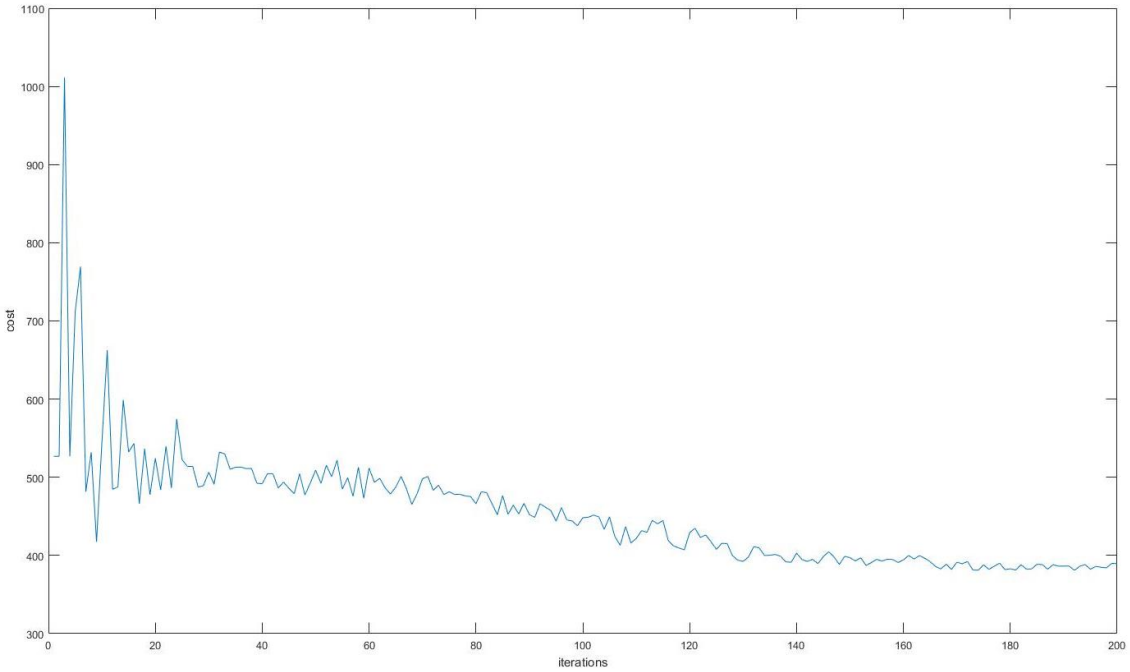

Figure 2.15: Plot of the cost with respect to number of iterations used in this thesis

Guidelines for SPSA:

As we already seen that there are lot of parameters to be specified for SPSA algorithm and some of the are as follows,

$$\lambda_j = \frac{\lambda}{(\lambda_0 + j)^{\alpha_1}}$$

Where $\lambda > 0$, $\lambda_0 > 0$, and $\alpha_1 > 0$, and

$$c_j = \frac{c}{j^{\alpha_2}}$$

where $c > 0$ and $\alpha_2 > 0$. However, if the θ_i have very different magnitudes, you may want to use different λ_j for each of the *p* dimensions. This can be difficult at times in practice, however, so another approach is to scale the parameter values themselves.

According to [1], some actual values that have been found useful in applications are

α_1 0.602 and α_2 = 0.101

Which are effectively the lowest allowable ones that satisfy theoretical conditions.

Step by Step working of SPSA:

1. All the values for λ, c, α_1, α_2 and number of steps are chosen.
2. A random initial value for θ is chosen, the thetaplus and thetaminus values for this particular θ are calculated at a distance of 'c' along with the respective costs.
3. Once the costs are known, the algorithm tries to move towards the lower cost with a step size of λ.
4. Then the values of λ and c are reduced. In other words, new values of λ and c are calculated based on the values of α_1, α_2
5. All these steps repeat until the values of λ and c become so small that the algorithm will not be able to move any further down the gradient.

Changes made to the normal SPSA algorithm:

All the steps explained above are for normal SPSA algorithm. But in this case the algorithm is a 4-D search space with lot of limitations. In this thesis, the priority was given for easy design of the robot than perfect energy optimization. This helps to mount the spring on the robot without additional work done on it or any other hassle.

The changes that were made to the search algorithm are as follows:

The equation for the final cost is given by

$$cost_{final} = I_\tau + \alpha_1 * \max(-preload, 0) + \alpha_2 * \max\big((maxl - lmax), 0\big) + \alpha_3 * abs\big(a_y\big) + \alpha_4 * abs(b_x)$$

where $'maxl'$ is the maximum allowable spring length; $'lmax'$ is the maximum length the spring extends during the stride. $'preload'$ is the extension on the spring on its mounting position and I_τ is given in section 2.1

1. Three extra parameters are added to the cost obtained from the *impulsefunction()*. They are '*preload', 'maximum allowable spring length'* and *'distance of AX and BX from origin'*

2. It is adjusted in such a way that, if *preload* is a negative the cost increases. To put it in better words, if the initial spring length is more than the *preload* we cannot install the spring.
3. Same goes with ‘maximum allowable spring length’. If the spring extends more than actual physical extendable limit of the spring in the simulation, the system breaks the spring, which is not feasible. If this value is negative the cost increases.
4. The parameter is used in order to make sure that one end of the spring stays on the leg rather going sideways from the leg. And the other end stays on the body of the robot rather going downwards from the body of the robot. More the distance from the origin, more is the cost.
5. The magnitude in which these three parameters increase in the cost is controlled by three different gains called *‘gsin1, gain2 and gain3’*.

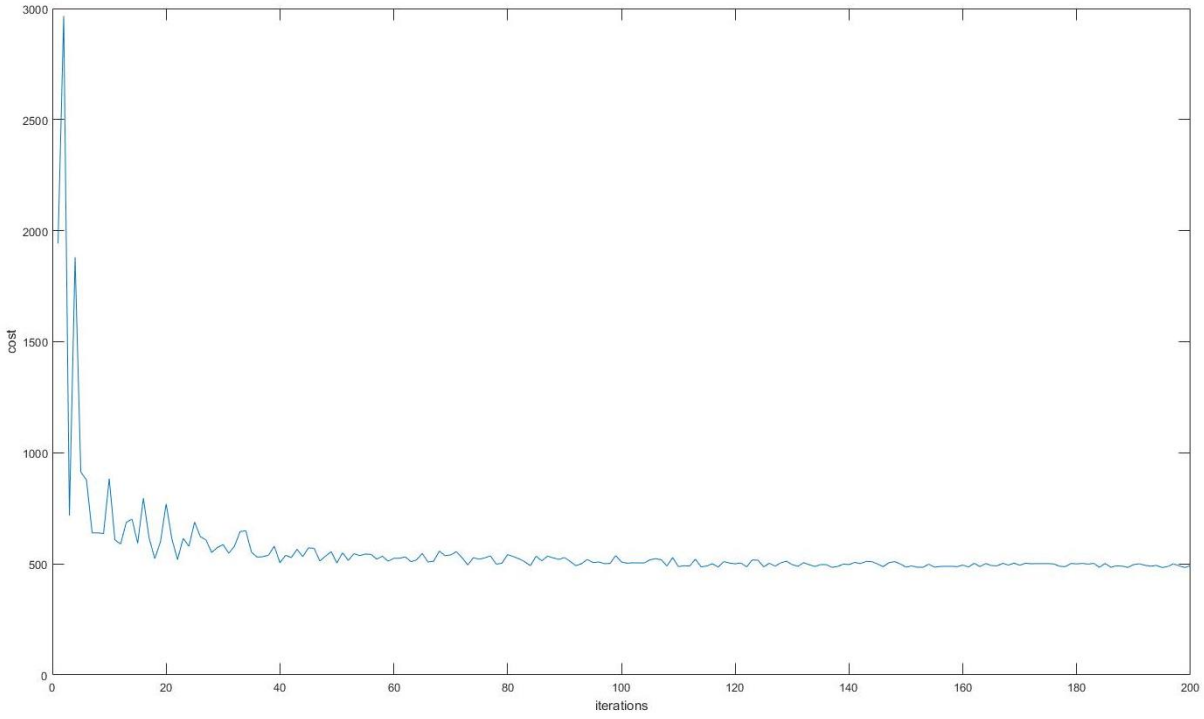

Figure 2.16: Plot of cost with respect to iterations after adjusting the parameters

2.3 RoboDynamics:

RoboDynamics is tool which helps us to simulate the physical effects on any kind of machine. This tool has flexibility to program which ever terrain needed. In this case, ***Random*** terrain, ***Flat*** terrain and ***Step*** terrain. This system samples the data every millisecond *(every thousandth of a sec).* This tool also offers various options to export the data that is required according to use. Few of the examples in this case are ***contact***, ***torque*** and ***angle*** of the leg during a complete step.

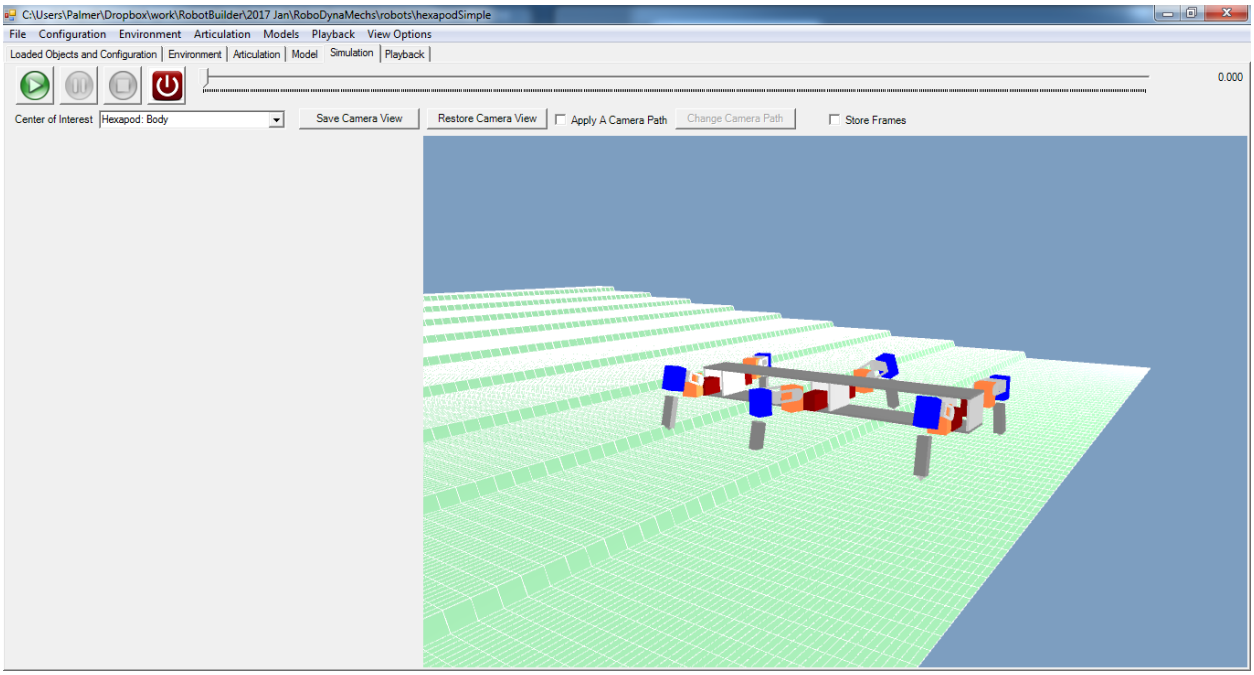

Figure 2.18: Figure which shows the user interface of the RoboDynamics tool

 : This button is used to start the simulation

 : This button is used to pause the simulation in middle

 : This button is used to stop the simulation. Once you hit this button all the data is exported

 : This button is used to turn on the simulation. Without this button we cannot start the simulation.

 : This slider is used to seek forward or reverse with respect to time of the simulation.

There are also various other options like *Loaded objects and configuration* which is used to define the robot's body and properties. If there are any other objects to be placed on the environment their properties are defined in this option itself.

To define the properties of the environment, say type of terrain, color of the terrain, height and depth of the terrain etc. can be defined using the *environment* option. The *playback* tab provides us with various options like location for the storage of the data, different types of parameters to be exported in the form of data etc.

The figures demonstrate what all terrain are used and how they look

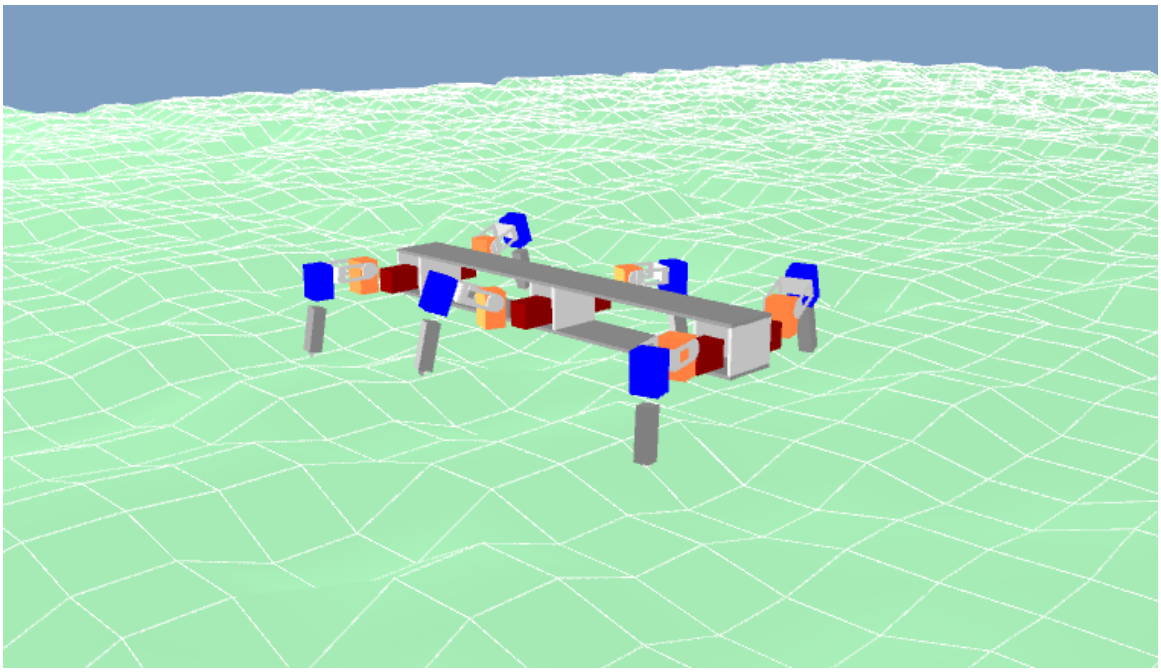

Figure 2.19: figure which shows the random terrain

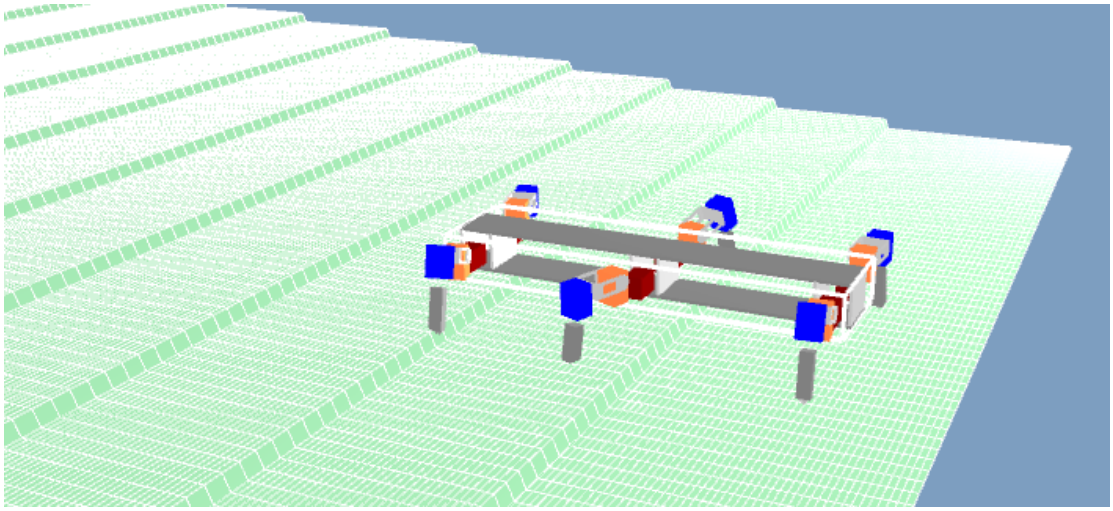

Figure 2.20: figure that shows step terrain

Chapter 3: Results

After using SPSA with 10 random initial points, and each point tested for 5 times, the obtained results for mounting position which is optimized both for energy and design is

AX = -0.0091m AY = -0.0079m

BX = -0.0066m BY = -0.0600m

Spring Stiffness = 1402.7659N/m Initial Length = 0.0508m

This spring can be found at www.mccmaster.com with a part number 9654K365

3.1 SPSA Results

When SPSA algorithm was performed on 2-D and 3-D search space, the results were accurate. There were no complications. But when the dimensions of the search space started increasing the results were not satisfactory. In order to figure out what makes the SPSA fail to work, the response surface of the *impulsefunction()* is plotted. But as our imagination is limited to three dimensions, one of the dimension is made constant and the response surface or the cost of the impulse function is plotted with respect to AX, AY, BY keeping BX constant. In this way, it is possible to look at the 3-D space of the response surface. The cost is defined according to color.

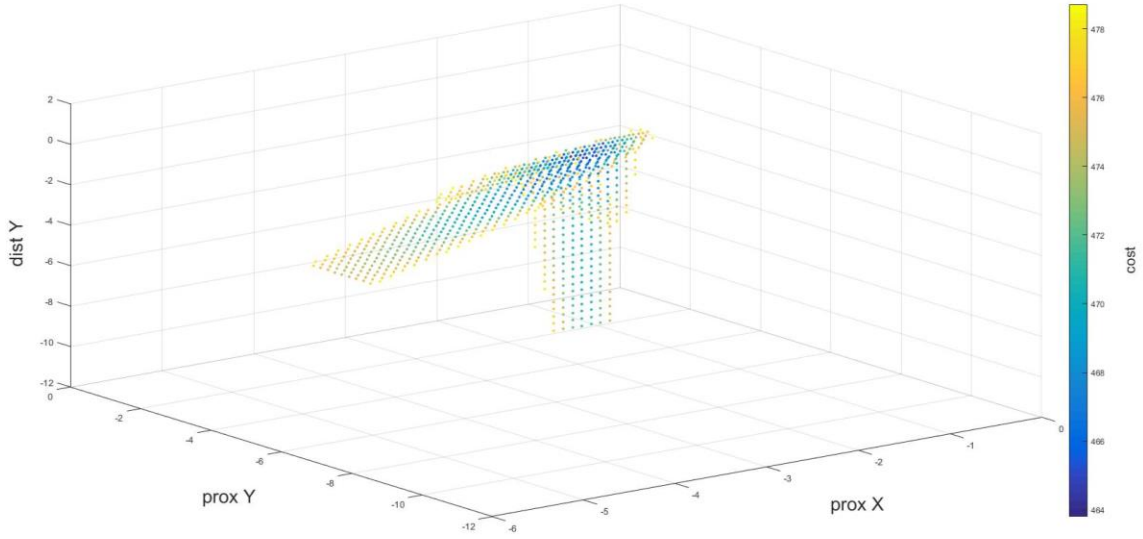

Figure 3.1: 3-D response surface BX = 0, and cost versus AX,AY on X and Y axis respectively and BY on Z axis

In the above figure, the range of the cost is given by a color bar on the right, where blue defines the lowest cost and yellow defines the highest cost. As it is clearly seen that there is a shelf kind of area in the plot. This shelf has the lowest gradient. Due to which the SPSA takes forever to reach the lowest point.

Let's say that the number iterations are 400, and It takes all 400 steps for the algorithm to reach some random point on the shelf (*as SPSA is a random algorithm*) then to reach to lowest point from that position it might even need more than a million steps. It is clearly seen in the system that there is minimum point, which could be the solution for this search *(point with the lowest cost)* which could be reached by more computations but at what cost? Even if we reach to the lowest point it might not be efficient, computational wise. So we resorted to the anchor points on the shelf which provide a cost that is in a range of 10% or 5% of the lowest point. If this is the case with three dimensions, then this ambiguity will continue to four dimensions too. Hence, we cannot get the same point or points that are close to the minimum all the time. This is where SPSA fails to get the exact solution (*which is a primary requirement for the algorithm to be considered successful*). The response surfaces of the cost with different BX values are also shown below.

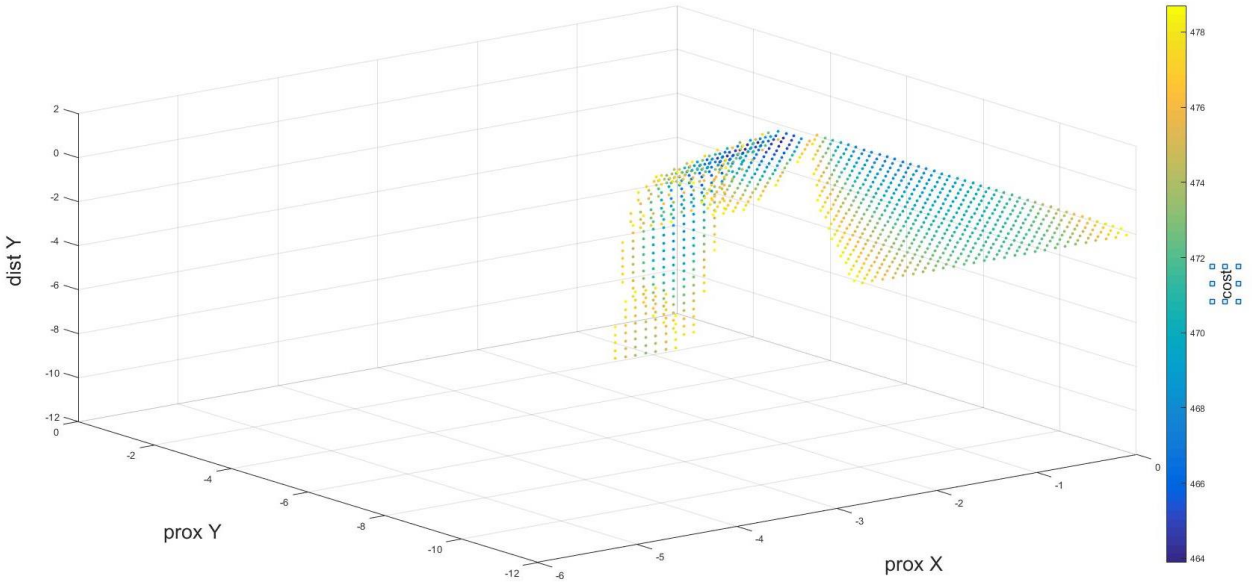

Figure 3.2: 3-D response surface at BX = 1cm, Cost vs BX, AX, AY

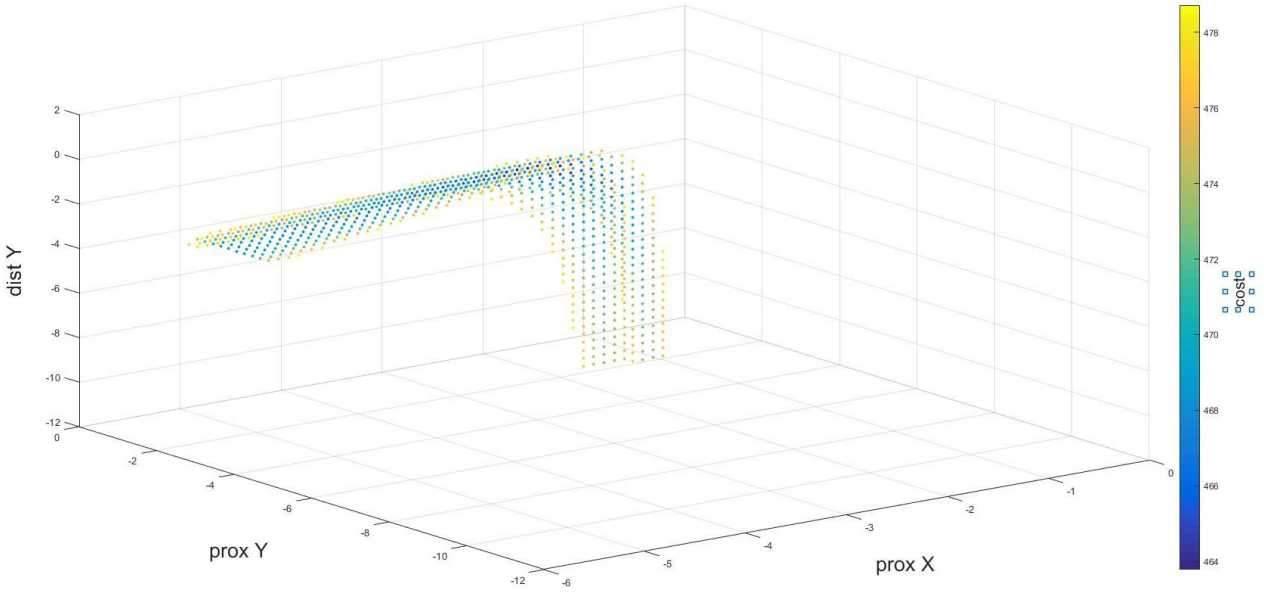

Figure 3.3: 3-D response surface at BX = -1cm, Cost vs BX, AX, AY

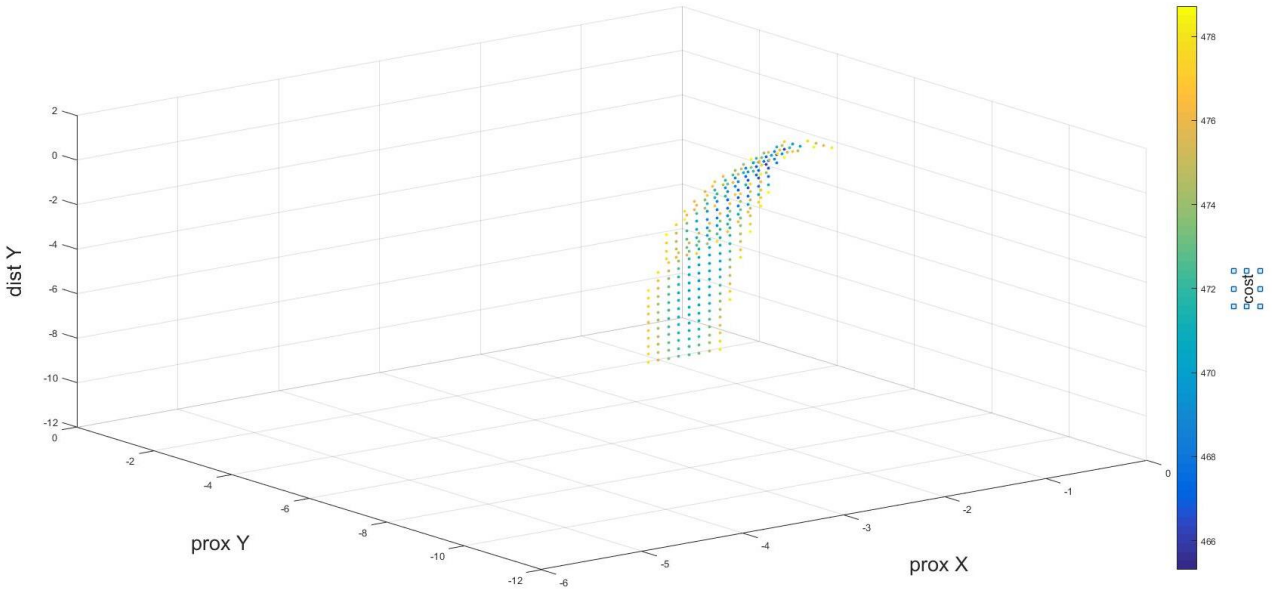

Figure 3.4: 3-D response surface at BX = 2cm, Cost vs BX, AX, AY

As seen in above figures, there is a similar shelf like pattern in all of them. This shelf is the reason why SPSA is unable to reach to the minimum point which we can be seen in all the cases. Due to this reason, instead of considering the lowest cost as the actual solution for the search, any point on that shelf is considered as the solution. This might not be completely efficient but relatively its better than being not able to find the spring that satisfies the solution. Moreover, the main priority in here is always given to the design than obtaining most efficiency for the dominant joint.

This small step back in the algorithm have made it possible to achieve much better design of the robot making the proximal and distal anchor of the spring stay on the body of the robot and on the leg of the robot respectively. All these adjustments are explained in the SPSA section (*chapter 2.2*) of this document. This about the 4-D search space of this algorithm. But there are also other two parameters that played a major role in obtaining the best possible result. One of them is ***Spring Stiffness.*** As we have already seen in case of 4-D search that the SPSA algorithm did not perform effectively and using the spring stiffness or the spring constant as the 5^{th} search parameter will make things even complex. To avoid this complexity instead of performing a gradient search on the spring stiffness,

all the specifications of the springs available in the market that would be helpful for the robot are logged in and the best suitable for the job are chosen. This gave a total number of 274 springs. From which only 76 where having the initial length that is required. Then these 76 combinations are processed through SPSA and the final result is obtained. Based on these factors the final solution i.e. the anchor points, the spring stiffness and the initial length of the spring are chosen. These results are shown in next section.

3.2 Walking Results:

After obtaining the results from SPSA algorithm, the particular coordinates for both the anchor points of the spring are given to the *impulsefunction()* along with other spring specifications like the *Spring stiffness* or *spring constant*. Depending on all these values the function gives an analysis of the torques and other factors during one complete stride period. The whole stride takes 2000 counts.

The various factors analyzed are shown in the figure below

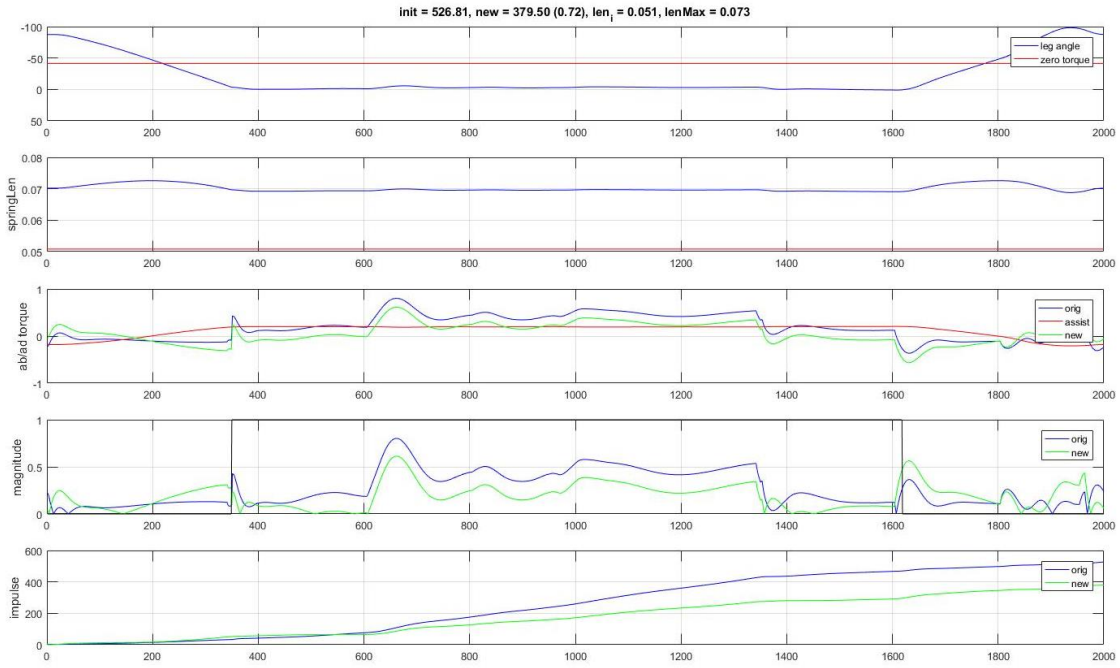

Figure 3.5: Step analysis of the results obtained from SPSA

Initial Torque: 526.81, New torque: 379.59, Efficiency: 28%, Initial Length: 0.051m, Max length: 0.073m, Zero Torque angle: -41.29º

To clearly understand each subplot, the individual plots are also shown below

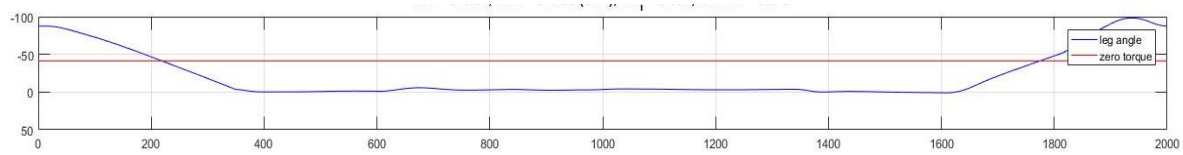

Figure 3.6: Zero torque angle = -41.29º

In the above figure is the plot of zero torque angle and the present angle of the motor or leg. ***Zero Torque Angle*** is a point at which the motor doesn't work against the spring force rather the spring force is nullified by the placement of the angle of leg itself. This is one point where we are saving some energy.

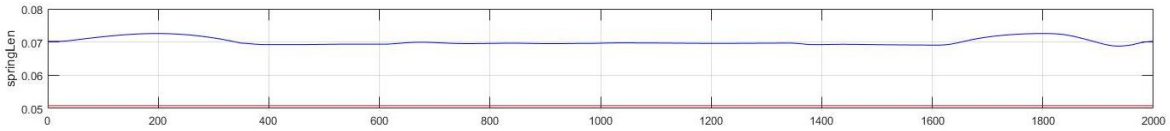

Figure 3.7: Extension of the Spring with respect to time

In this figure, the initial spring length is shown in black color and the present spring length is shown in blue color. This figure gives a clear understanding of the stress applied on the spring during different phases of the stride.

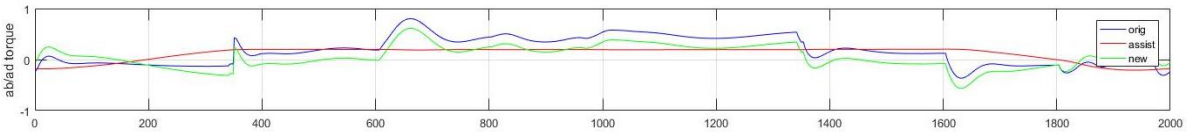

Figure 3.8: Plots of various torques with respect to time

This figure shows the torque applied by the motor, force applied by the spring and the total torques ie the summation of the motor torque and the spring force. The blue line is the original torque applied by the motor, the red line is the force applied by the spring and the yellow line is the total torque. The direction of these torques also play a major role in this figure. The torques in the same direction and the new torque less than the original torque means the spring is helping the system and the if the directions are opposite with same

values then the spring is hurting the system. If opposite direction and the blue line is less than the yellow line, then the spring is helping the system. To make things easy, the magnitude plot of the above figure is also shown in next figure.

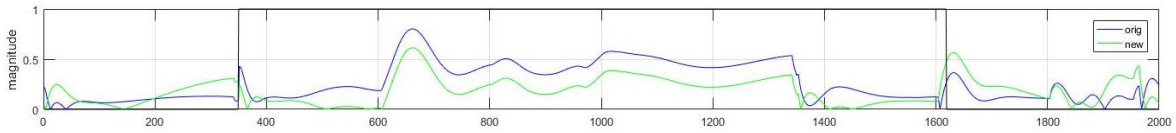

Figure 3.9: Magnitude plot of various torques along with the contact vector

This figure contains the magnitude plots of all the torques. The blue line is the original torque, the yellow line is the new torque and the black rectangular box kind of line is the contact of the leg with the ground. If the value is 1, then robot is in *Stance* phase. If its '0' then the robot's leg is in *Swing* phase.

Finally, there is this plot of summation of the overall torque through the whole stride period and this is shown in the next figure.

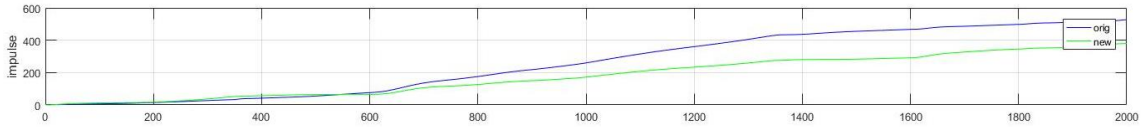

Figure 3.10: Integral of all the torques

Blue line is the original torque and the yellow line is the new torque. If the blue line is greater than the yellow line, that indicates that the spring is helping the system during the overall stride period.

Flat Terrain:

During all testing and walking the robot only followed one gait which is tripod gait. The tripod gait follows a constant pattern during all the steps.

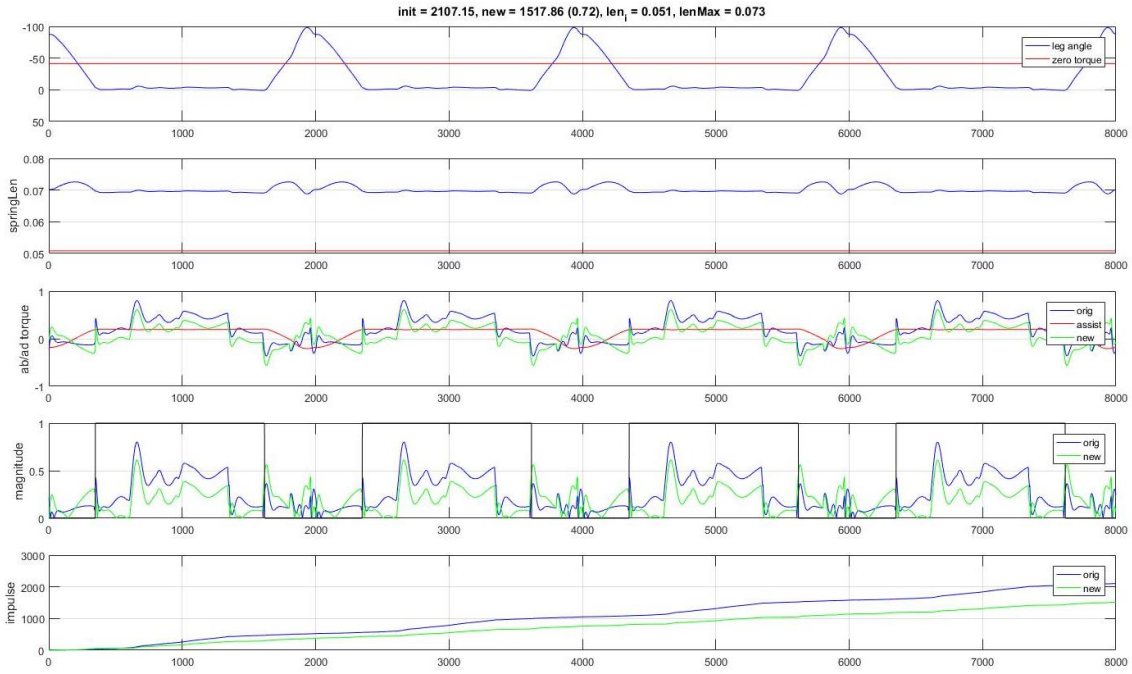

Figure 3.11: Analysis of different factors, while robot walks 4 steps

Initial torque: 2107.15 N.m, New torque: 1517.86 N.m, initial length of spring: 0.051m, maximum extended length of spring: 0.073, Zero torque angle: -41.29º, efficiency: 28%

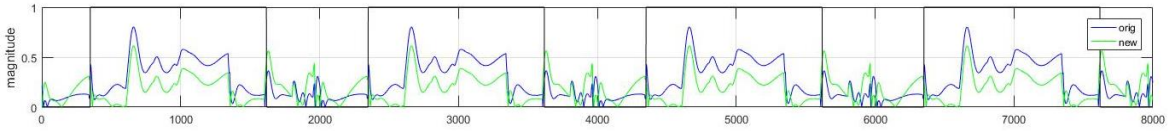

Figure 3.12: Subplot of Magnitude of various torques along with the contact vector during all 4 steps

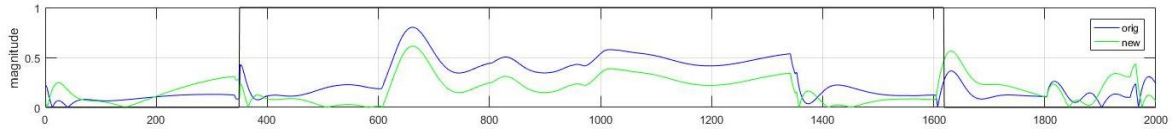

Figure 3.13: Plot of Magnitude of various torque along with contact vector during single step.

Here we can see that at 370milliseconds the leg contacts the ground i.e. the robot goes into stance phase, at this point all the weight of the robot is on the leg. Now, the spring force comes into play and supports the body weight making the motor exert less torque. This is

where most of the energy is saved. If say, the duty cycle of the stride is 75% i.e. the robot stays in stance phase for 75% of the stride period then all the energy required to generate torque that can support the body weight during this time is saved. The other time i.e. before 370milliseconds and after 1600 milliseconds the leg stays in the air. During this time, all the weight of the leg must be supported by the motor and also the spring force acts against the motor torque. All this together makes the total torque higher than the original torque. Also, there is one point where spring force doesn't work against the motor torque even though the leg is in swing phase. That point is called the Zero torque angle.

Upward Stairs:

Analysis of the results on step up terrain

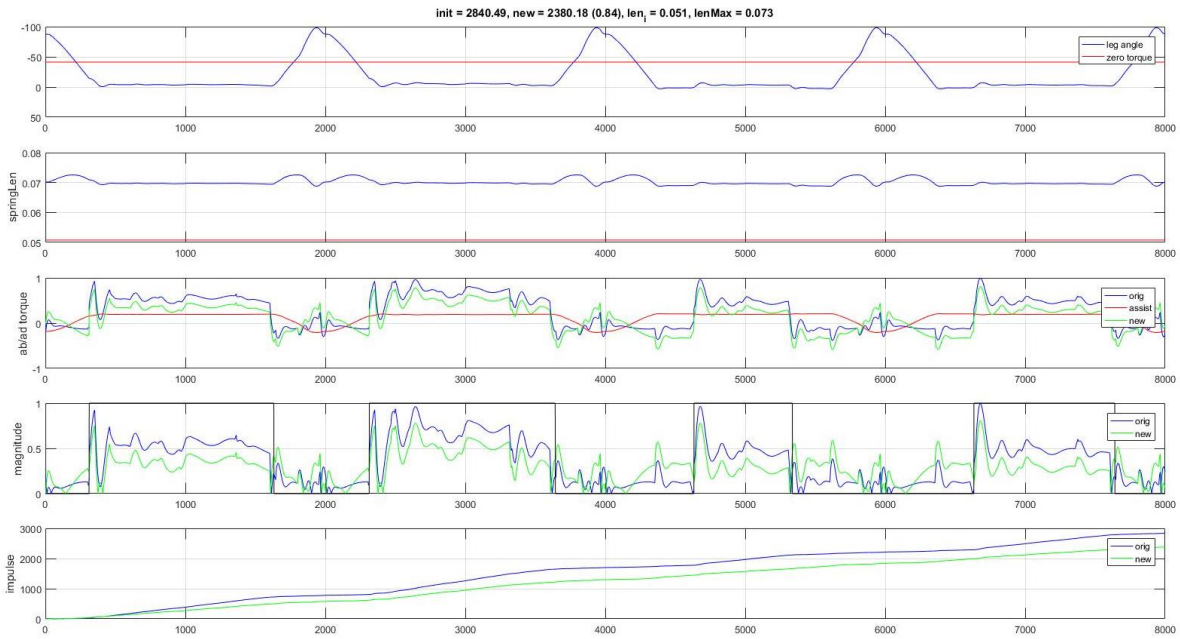

Figure 3.14: Analysis of different factors on step up terrain for 4 steps

Initial Torque: 2840.49 N.m, New torque: 2380.18 N.m, Efficiency: 16%, Initial length of spring: 0.051m, Maximum extension of spring: 0.073m, Zero Torque angle: -41.29º

The Efficiency of the system decreased from flat terrain to stair case. The reason for this drop in the efficiency can be observed in subplot 4 of the above figure from 4000milliseconds to 6000 milliseconds. Although the robot is following the same tripod gait but the stance phase of leg decreased. This is because during that step, the other legs

of the robot could take over the weight as the found the ground faster due to the stair case terrain. This made the motor to take all the load of the leg and the spring force. To do so, the motor must require more torque due to which new torque was 1.05% more than the original torque.

Random Terrain:

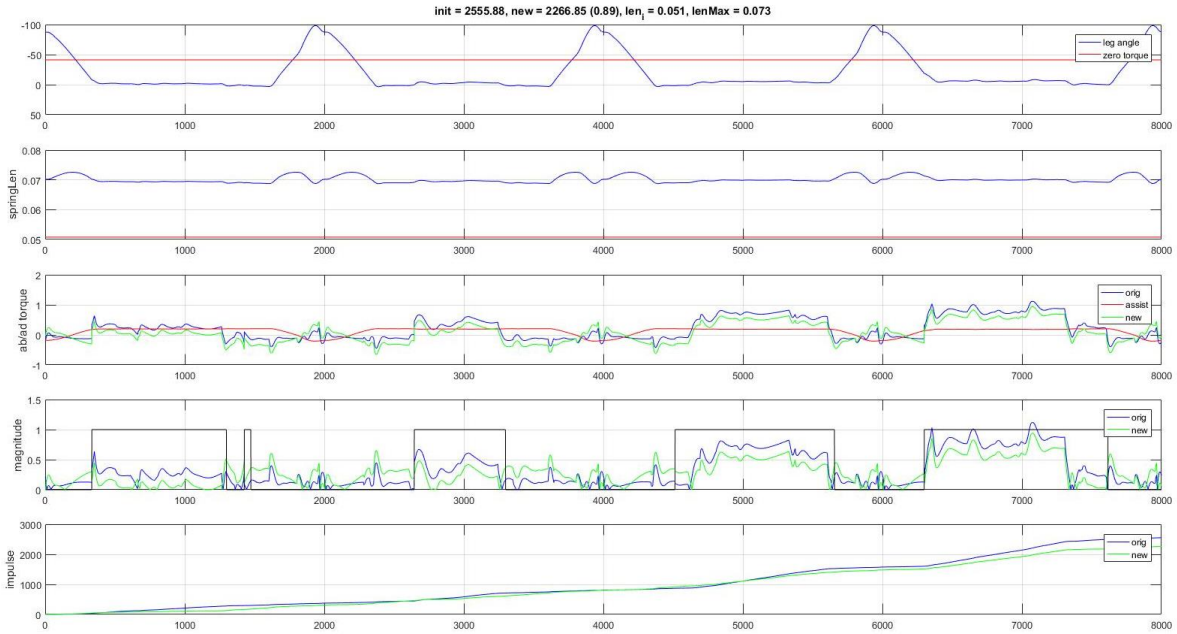

Figure 3.15: Analysis of the various factor on random terrain for 4 steps

Initial Torque: 2555.88 N.m, New Torque: 2266.85 N.m, Efficiency: 11%

As same spring is being used, the initial length of the spring, maximum extension of the spring and the zero-torque angle will all be same as before. But the difference in efficiency is due to the randomness of the uneven terrain. During the step from 0 milliseconds to 2000 milliseconds, the stance phase completed way before the normal time, and then immediately the leg contacted the ground at 1500milliseconds for a small amount of time. This randomness of the terrain caused the leg to stay in air even though it is in stance phase. This uncertainty in the time period of the stance phase and the leg contacting the ground made the motor to take all the load of both leg and spring force.

Chapter 4: Future Work:

Number of legs used:

All the data gathered and tested is based on single leg, Leg number #2. The results obtained from the single leg are used on all the legs which might be better unless the gait pattern doesn't change. But if the gait changes, then using same results for all the legs might not be feasible. Future work could be gathering data for individual leg and finding a solution for each leg and then testing those solutions.

Different gaits used:

Throughout the work, the only gait used is the *Tripod Gait.* No other gait is tested. The results obtained might work even better for other gaits like wave gait. Or the results obtained by using the data obtained from other gaits might prove to be more efficient. Future work will be adopting these results on all the legs with multiple gaits.

Multiple Terrain:

In this thesis, the testing is done on single terrain at a time. The data used for searching the solution was obtained from flat terrain tripod gait walking. The same solution obtained can be used on multiple terrain like changing from flat terrain to random terrain with starting the simulation again.

Hardware:

Due to few reasons, the testing was done only on software. In the future, the obtained spring specifications and the mounting points can be used on a the real hexapod shown before and the power consumption of the robot can be analyzed.

The Big Picture:

Once this system is tested on the hardware with multiple gait patterns, multiple terrains and based on the results it can be adopted to almost all kind of walking robots. This system can be made universal. This thesis didn't talk about the effect on the stability of the robot. One can also analyze the stability of the robot when this system is used.

Chapter 5: References

[1] Firas A. Raheem, Hind Z. Khaleel, ”Static Stability Analysis of Hexagoanl Hexapod Robot for periodic gaits”, *IJCCCE* ,Vol. 14, No. 3, 2014

[2] Types of Robot Gait. (n.d.). Retrieved July 27, 2017, from http://hexapodrobots.weebly.com/types-of-robot-gait.html

[3] Saranli, U.; Buehler, M.; Koditschek, D.E. (2001). "RHex: A Simple and Highly Mobile Hexapod Robot". *The International Journal of Robotics Research*. **20** (7): 616.

[4] Aaron M. Hoover, Samuel Burden, Xiao-Yu Fu, S. Shankar Sastry, and R. S. Fearing (2010).” Bio-inspired design and dynamic maneuverability of a minimally actuated six-legged robot” International Conference on Biomedical Robotics and Biomechatronics.

[5] LAURON V: A Versatile Six-Legged Walking Robot with Advanced Maneuverability. IEEE/ASME International Conference on Advanced Intelligent Mechatronics (AIM 2014), At Besançon, France.

[6] Roennau, Arne; Heppner, Georg; Pfotzer, Lars; Dillmann, Ruediger (July 2013). "LAURON V: Optimized Leg Configuration for the Design of a Bio-Inspired Walking Robot".

[7] Passino, K. (2005). Biomimicry for optimization, control, and automation. London: Springer.

[8] D. E. Goldberg: Genetic Algorithm in Search Optimization, and Machine Learning, Addiso Wesley, 1989.

[9] Sigeyasu Kawaji and Kazufumi Sawasa: DYTION ROBOT WITH CHARACTERUSTIC RHYTHM, JAPAN/USA Symposium on Flexible Automation-Volume 1 ASME 1992

[10] Ahmed, M., M.M. Billah, M.R. Khan and S. Farhana, 2009. Walking hexapod robot in disaster recovery: Developing algorithm for terrain negotiation and navigation. J. World Acad. Sci. Eng. Technol., 42: 328-333. http://www.waset.com

[11] IEEE and Fraunhofer, 2008. IPA database on service robotics-reconstruction. (n.d.). Retrieved July 27, 2017, from http://www.ipa.fhg.de/srdatabase/rosy.html

[12] Jun Nishii, Legged insects select the optimal locomotor pattern based on the energetic cost, Biological Cybernetics, October 2000, Volume 83, Issue 5, pp 435–442

[13] Nishii, J. Biol Cybern (2000) 83: 435. https://doi.org/10.1007/s004220000175, Springer-Verlag, 0340-1200

[14] Yasuhiro Fukuoka, Kota Fukino, Yasushi Habu and Yoshikazu Mori, Journal: Bioinspiration & Biomimetics, 2015, Volume 10, Number 4, Page 046017

[15] Taniai, Y., & Nishii, J. (2006). Optimality of the minimum endpoint variance model based on energy consumption. International Congress Series, 1291, 101-104. doi:10.1016/j.ics.2006.01.049

[16] Scarfogliero, U., Stefanini, C., & Dario, P. (2009). The use of compliant joints and elastic energy storage in bio-inspired legged robots. Mechanism and Machine Theory, 44(3), 580-590. doi:10.1016/j.mechmachtheory.2008.08.010

[17] Jiang, W. Y., Liu, A. M., & Howard, D. (2004). Optimization of legged robot locomotion by control of foot-force distribution. Transactions of the Institute of Measurement and Control, 26(4), 311-323. doi:10.1191/0142331204tm124oa

[18] Gardner, J. F., Srinivasan, K. and Waldron, K. J. 1990: A solution for the force distribution problem in redundantly actuated closed kinematic chains. Journal of Dynamic System, Measurement and Control, Transactions of the ASME 112, 523-526.

[19] Kar, D. C., Issac, K. and Jayarajan, K. 2001: Minimum energy force distribution for a walking robot. Journal of Robotic Systems 18, 47-54

[20] Kumar, V. R. and Pugh, D. R. 1988: Force distribution in closed kinematics chains. IEEE Journal of Robotics and Automation 4, 657-663

[21] Orin, D. E., & Oh, S. Y. (1981). Control of Force Distribution in Robotic Mechanisms Containing Closed Kinematic Chains. Journal of Dynamic Systems, Measurement, and Control, 103(2), 134. doi:10.1115/1.3139653

[22] Santos, P. G., Garcia, E., Ponticelli, R., & Armada, M. (2009). Minimizing Energy Consumption in Hexapod Robots. Advanced Robotics, 23(6), 681-704. doi:10.1163/156855309x431677

[23] Huang, Q., Hase, T. and Ono, K. 2007. Optimal trajectory planning method using inequality state constraint for biped walking robot with upper body mass, Special Issue on New Trends of Motion and Vibration Control. J. Syst. Des. Dyn. (JSME Dyn. Meas. Control Div.), 1: 168–179

[24] Nahon, M. A. and Angeles, J. 1992. Minimization of power losses in cooperating manipulators. J. Dyn. Syst. Meas. Control, 114: 213–219.

[25] Bares, J. E. and Wettergreen, D. S. 1999. Dante II: technical description, results and lesson learned. Int. J. Robotics Res., 18: 621–649.

[26] Hector Montes, Lisbeth Mena, Roemi Fernández, Manuel Armada. (2017) Energy-efficiency hexapod walking robot for humanitarian demining. Industrial Robot: An International Journal 44:4, pages 457-466.

[27] Silva, M. F., & Machado, J. T. (2011). A literature review on the optimization of legged robots. Journal of Vibration and Control, 18(12), 1753-1767. doi:10.1177/1077546311403180

[28] Ahmadi M and Buehler M (1999) The ARL monopod II running robot: control and energetics, in Proceedings of the 1999 IEEE International Conference on Robotics and Automation, Detroit, MI, May 10–15, pp. 1689–1694

[29] Juárez-Guerrero J, Muñoz-Gutiérrez S and Cuevas WWM (1998) Design of a walking machine structure using evolutionary strategies. In Proceedings of the 1998 IEEE International Conference on Systems, Man and Cybernetics, 11-14 October 1998, San Diego, CA, pp. 1427–1432

[30] Lapshin VV (1995) Energy consumption of a walking machine. model estimations and optimization, in Proceedings of ICAR'95 – Seventh International Conference on Advanced Robotics, September 1995, Sant Feliu de Guixols, Catalonia, Spain, pp. 420–425

[31] Neuhaus P and Kazerooni H (2000) Design and control of human assisted walking robot, in Proceedings of the 2000 IEEE International Conference on Robotics and Automation, 24-28 April 2000, San Francisco, CA, pp. 563–569